Evaluation of two fungal exopolysaccharides as potential biomaterials for wound healing applications

Masoud Hamidi[1,2], Oseweuba Valentine Okoro[1], Khodabakhsh Rashidi[3], Mohammad Saeid Salami[3], Rasool Mirzaei Seveiri[2], Hadi Samadian[4,*], Amin Shavandi[1,*]

[1] Université libre de Bruxelles (ULB), École polytechnique de Bruxelles, 3BIO-BioMatter, Avenue F.D. Roosevelt, 50 - CP 165/61, 1050 Brussels, Belgium

[2] Department of Medical Biotechnology, Faculty of Paramedicine, Guilan University of Medical Sciences, Rasht, Iran

[3] Research Center of Oils and Fats, Research Institute for Health Technology, Kermanshah University of Medical Sciences, Kermanshah, Iran

[4] Dental Implants Research Center, Hamadan University of Medical Sciences, Hamadan, Iran

*** Correspondances:**

Hadi Samadian
Dental Implants Research Center, Hamadan University of Medical Sciences, Hamadan, Iran
Email: h30samadiyan@gmail.com

Amin Shavandi
Université libre de Bruxelles (ULB), École polytechnique de Bruxelles-BioMatter unit, Avenue F.D. Roosevelt, 50 - CP 165/61, 1050 Brussels, Belgium Amin.Shavandi@ulb.be

Abstract

Microbial exopolysaccharides (EPSs) are mostly produced by bacteria and fungi and have potential use in nutraceuticals, medicine, and industry. The present study investigated the *in vitro* biological activities and *in vivo* wound healing effects of EPSs produced from a Sclerotium-forming fungus *(Sclerotium glucanicum* DSM 2159) and a yeast (*Rhodosporidium babjevae),* denoted as scleroglucan (Scl) and EPS-R, respectively. EPS yields of 0.9 ± 0.07 g/L and 1.11 ± 0.4 g/L were obtained from *S. glucanicum* and *R. babjevae*, respectively. The physicochemical properties of the EPSs were characterized using infrared spectroscopy and scanning electron microscopy. Both EPSs were cytocompatible toward the human fibroblast cell line and showed hemocompatibility. Wound healing capacities of the EPSs (10 mg/mL) were also determined *in vivo*. EPSs produced by *S. glucanicum* and *R. babjevae* have the potential as biocompatible components for dermal wound healing.

***Keywords*:** Exopolysaccharide (EPS); *Rhodosporidium babjevae*, Scleroglucan; *Sclerotium glucanicum*; Wound healing

Introduction

Several strains of fungi and bacteria secrete exopolysaccharides (EPSs) to the surrounding environment (El-Ghonemy 2021). These EPSs are homo- or hetero- long-chain branched biopolymers that are composed of monosaccharides (i.e., glucose) and inorganic constituents such as sulfate, phosphate, and acetyl, in the side chains, in varying compositions (Decho and Gutierrez 2017; Sathishkumar et al. 2021). EPSs are involved in a variety of physiological processes and functions such as protection of microbial cells from unfavorable environmental conditions (i.e., exposure to ultraviolet (UV) irradiation and toxic compounds), biofilm construction, nutrition acquisition, stress resistance, and antimicrobial resistance (Masoud Hamidi et al. 2018; Pirhanov et al. 2021; Sajna et al. 2021). EPSs are mainly produced by bacteria and fungi (Mahapatra and Banerjee 2013; Hamidi et al. 2022a) with fungi considered as a preferred EPS source due to their low production cost, sustainability, and low environmental influences, and biodegradability. Indeed, the advantages of fungal EPSs highlight their potential to compete favorably with biopolymers acquired from higher plants, marine algae, and synthetic polymers. Additionally, fungal EPSs are characterized by short production times (e.g., within a few days), simple recovery approaches and can be generated by industrial waste such as glycerol, hydrocarbon residue, and CO_2, as carbon sources (Elsehemy et al. 2020a; Okoro et al. 2021).

The structural composition and habitat of the host-microbe determine the specific roles of microbial EPSs. Furthermore, studying the content and structure of EPSs is necessary to assess their potential applications (Rana and Upadhyay 2020). Notably, variations in fungal EPSs compositions facilitate differences in structural, physicochemical properties and their biological effects with EPSs containing β-D-glucans recognized as biological response modifiers (BRMs) (Geller and Yan 2020; Han et al. 2020; Jaroszuk-Ściseł et al. 2020). BRMs are agents that can affect the normal immune response, with cytokine induction being one of the main modes of action (Chatterjee et al. 2018). For instance, Kwon et al. assessed the wound healing efficacy of β-glucan extracted from *Sparassis crispa* in diabetic rats and observed enhanced wound healing and increased macrophage infiltration into the wound bed (Kwon et al. 2009). In addition, it was shown that EPSs containing mannose (mannans), could also function as potential BRMs (Liu et al. 2021b; Hamidi et al. 2022b) due to the presence of the mannose receptors on macrophages and dendritic cells (Apostolopoulos and McKenzie 2001).

Scleroglucan (Scl) is a β-D glucan, which consists of β-(1→3)-linked glucose with a β-(1→6)-glycosyl branch on every third unit. It is a water-soluble EPS produced by fungi of the genus *Sclerotium*. i.e., *Sclerotium glucanicum, Sclerotium rolfsii* and *Sclerotium delphinii* (Elsehemy et al. 2020a; Zeng et al. 2021). Scl has various applications in the oil, food, pharmaceutical, and cosmetic industries (Mahapatra and Banerjee 2013;

Keshavarz et al. 2022). Scl solutions are stable at temperatures up to 100–120℃ and throughout a wide pH range (1–13) (Viñarta et al. 2013). Furthermore, the neutral nature of EPS permits it to maintain pseudo-plasticity even in the presence of salts such as NaCl, KCl, $CaCl_2$, $MgCl_2$, and $MnCl_2$ (Viñarta et al. 2013). The use of Scl as an antitumor, antiviral, antimicrobial, immune-stimulating, hypocholesterolemic and hypoglycemic, as well as a drug-delivery vehicle agent, has also been reported (Pretus et al. 1991; Valdez et al. 2019). For instance, Elsehemy et al. showed that Scl extracted from *Athelia rolfsii* TEMG, at 15 and 50 ng/mL of herpes simplex virus type-1 (HSV-1) and influenza viruse (H5N1), respectively, was able to reduce the cytopathic effect by 50% (EC_{50}) (Elsehemy et al. 2020b).

Rhodosporidium babjevae with the ability to thrive in nutrient (i.e., nitrogen) deficient environments and produce mannose-rich EPS has been selected as the preferred yeast microorganism. (Sitepu et al. 2013). *R. babjevae* was initially isolated from herbaceous plants in Moscow, Russia as a red-pigmented, non-ballistosporogenous yeast with the EPS characterized by a monosaccharide composition of mannose (>80 mol%) and glucose (Mirzaei Seveiri et al. 2020). Also, in our previous work, it was shown that the EPS from *R. babjevae* (called EPS-R in this study), has emulsifying and antioxidant activities and was biocompatible toward Madin-Darby Canine Kidney (MDCK) cell line (Mirzaei Seveiri et al. 2020).

Therefore, due to the potential of β-glucans and mannans to be used as a therapeutic agents the current study, seeks to comparatively assess the biological and wound healing performances of Scl (representative of a β-glucan) and EPS-R (representative of a mannan polymer), obtained from *S. glucanicum* and *R. babjevae*, respectively. Also, it is worth mentioning that this study seeks, for the first time, to assess the *in vivo* wound healing effects of Scl and an EPS from *Rhodosporidium* genus.

Materials and methods

Materials and reagents

Potato dextrose broth (PDB) was purchased from HiMedia, India (Model Number: M403-100G). Agar (CAS number: 9002-18-0) was obtained from AppliChem, Germany. Sucrose (CAS number: 57-50-1) was purchased from Fisher Chemical, Belgium. Magnesium sulfate heptahydrate (CAS number: 10034-99-8), yeast extract (CAS number: 8013-01-2), and 1,1-diphenyl-2-picrylhydrazyl (DPPH) (CAS number: 1898-66-4) were purchased from Merck (St. Louis, MO, USA). Ethanol (96%) (CAS number: 64-17-5) was obtained from Avantor®, Belgium. RealTime-Glo™ MT Cell Viability Assay kit was purchased from Promega, Madison, WI, USA (catalog number: G9711). Commercial Scl was purchased from Biosynth Carbosynth, UK.

Microorganisms and inoculum preparation

S. glucanicum DSM 2159 was acquired from the German Collection of Microorganisms and Cell Cultures GmbH (DSMZ), Braunschweig, Germany. It was cultured in the recommended medium of DSMZ (malt extract peptone agar) at 24 ˚C. To inoculate 100 mL of the basal medium, two agar discs of well-grown fungal culture (9 mm in diameter) were utilized (Selbmann et al. 2002) with some modifications for the inoculum preparation: D-glucose 30 g/L; $NaNO_3$ 3 g/L; yeast extract 1 g/L; $MgSO_4.7H_2O$ 0.5 g/L; KH_2PO_4 1 g/L; citric acid 0.7 g/L; and ferrous sulfate 0.05 g/L, pH 4.5 in 250 mL Erlenmeyer flasks. The medium was then incubated at 28℃, 150 rpm for 72 h on a rotary shaker (New Brunswick Classic C24 Incubator Shaker, USA).

The *R. babjevae* (IBRC-M 30088; equivalent to ATCC 90942), was provided by Dr. Jafar Amani (Professor at Applied Microbiology Research Center, Baqiyatallah University of Medical Sciences, Tehran, Iran). The *R. babjevae* single colonies were inoculated into a potato dextrose broth (PDB) medium and incubated for 48 h (180 rpm at 28 ˚C). The 48 h old culture, was harvested and used as the inoculum at a concentration of 8% (v/v) in all experiments (Mirzaei Seveiri et al. 2020). The basal medium for EPS production contained 30 g/L glucose, 2.5 g/L $(NH_4)_2SO_4$, 1 g/L KH_2PO_4, 0.5 g/L $MgSO_4.7H_2O$, 0.1 g/L NaCl, 0.1 g/L $CaCl_2.2H_2O$ and 3 g/L yeast extract. The medium's primary pH was adjusted to 5.5 (Ghada et al. 2012; Mirzaei Seveiri et al. 2020).

EPSs extraction and purification

The Scl was recovered and extracted according to the protocol reported in the literature (Elsehemy et al. 2020a) with slight modification. Briefly, the broth culture was initially homogenized in a mechanical blender for 5 min after which it was neutralized to pH 6.5–7 using NaOH solution (0.1 N). The neutralized culture was then diluted with distilled water (2:1 v/v) and heated in a water bath at 90 ˚C for 1 h to precipitate any protein present in the culture medium. After cooling, the broth was centrifuged (3K3 centrifuge, Sigma Laboraxentrifugen, Germany) at 12000 rpm for 20 min. The Scl was precipitated from the clear supernatant by the addition of cold ethanol (96 v/v%) with a volumetric ratio of cold ethanol to the supernatant of two employed. This mixture was then stored overnight at 4 ˚C to ensure complete Scl precipitation. The crude Scl obtained by sieving was then resuspended in distilled water and further purified by cold ethanol re-precipitation (twice). The obtained Scl was then freeze-dried (Christ freeze-dryer alpha I-5) and the mass of the dried Scl was obtained using a precision analytical balance (Sartorius 1702MP8, Germany) with the yield of Scl calculated and reported in g/L. For EPS extraction and purification from *R. babjevae* (EPS-R), the methods reported in the literature (Mirzaei Seveiri et al. 2020) with slight modifications were employed. After incubation, centrifugation at 8500 rpm (15 min, 4 ˚C) was employed to recover the EPS-R supernatant. The recovered EPS-R supernatant was precipitated by adding

two volumes of cold ethanol dropwise while stirring. The mixture was then stored at 4 ˚C for 24 h. The precipitated EPS-R was then 'washed' twice using cold ethanol (8500 rpm centrifugation for 12 min at 4 ˚C), to facilitate EPS-R precipitate recovery. To produce dried EPS-R pellets, the recovered EPS-R precipitate was then dried at room temperature to constant mass. The EPS-R pellets were dissolved in distilled water and centrifuged at 8500 rpm for 20 min at 4 ˚C and the EPS-R supernatant was recovered. The EPS-R was then recovered, dried and the yield was measured using similar methods to the Scl recovery methods discussed earlier. The total carbohydrate content of the extracted Scl and EPS-R were also determined using the phenol-sulphuric acid method with glucose utilized as the standard (Dubois et al. 1956).

Scanning electron microscopy and Fourier transform infrared (FT-IR) spectroscopy

The surface morphology and microstructure of the Scl were determined by coating 5 mg of the Scl sample with gold and then using the scanning electron microscope (SEM) (SU-70 Hitachi Ltd., Tokyo, Japan), operating with an accelerated voltage of 10–20 kV. Also, at room temperature, an Infrared Spectrometer (Jasco brand model FT/IR-6600, integrated with Spectra ManagerTM II Software) was used to obtain the FT-IR spectrum of Scl and the EPS-R in the wavelength region of 4000 to 400 cm^{-1}, with a 4 cm^{-1} spectral resolution. Since the SEM images of the EPS-R have been reported in our previous report (Mirzaei Seveiri et al. 2020), SEM investigations were not undertaken in the current study.

***In vitro* biological activities**

Antioxidant activity

The antioxidant activity of the produced Scl was assessed according to the method in the literature (de Torre et al. 2019). The method involves the measurement of the free radical (DPPH•) scavenging activities of different concentrations (0.1, 0.25, 0.5, 1, 2.5, and 5, mg/mL) of Scl in distilled water. L-ascorbic acid was employed as a positive control due to its strong free radical scavenging ability. Briefly, different concentrations of 150 µL of the Scl sample in distilled water were combined with 150 µL of DPPH methanol solution (100 µM) and placed into different 96 well plates. The well plates were then incubated at room temperature for 40 min. Using a UV–Vis Spectrophotometer (Microplate spectrophotometer, Epoch-BioTek, Winooski, USA), the absorbance of the combination was measured at 517 nm, and the percentage of DPPH inhibitory activity (*inhibition*%) of the Scl solutions was calculated as follows;

$$Inhibition\% = \left(1 - \left(\frac{Abs_s - Abs_{sb}}{Abs_c - Abs_b}\right)\right) 100 \quad (1)$$

where Abs_s represents the absorbance of the sample (Scl in water and DPPH solution), Abs_{sb} represents the absorbance of the blank sample (Scl in water + methanol), Abs_c denotes the absorbance of the control (methanol + DPPH) and the Abs_b denotes the absorbance of the blank (methanol only).

Hemocompatibility test

2 mL of anticoagulated human red blood cells (RBCc) was diluted with 2.5 mL of PBS (stock solution) and 200 µL of this mixture was used in the preparation of Scl and the EPS-R solutions at different concentrations (1, 5, and 10 mg/mL). The mixture was then incubated at 37 ˚C for 60 min. The incubated RBCs + Scl/EPS-R solutions were then centrifuged at 1500 rpm for 5 min and the absorbance of the supernatant sample was measured at the wavelength of 545 nm using a BioTek absorbance microplate reader (ELX800, BioTek Instruments, Inc., Winooski, VT, USA). The hemolysis percent (*He*%) was then determined as follows (Ai et al. 2019);

$$He\% = \left(\frac{D_t - D_{nc}}{D_{pc} - D_{nc}}\right) 100 \quad (2)$$

where D_t is the absorbance of the supernatant sample, (Au), D_{nc} is the absorbance of the negative control (blood diluted with PBS), (Au) and D_{pc} is the absorbance of the positive control (water lysed RBCs), (Au).

Effect of the EPSs on the viability of human fibroblast cell line

Different concentrations of the Scl (400, 600, 800, and 1000 µg/mL) and the EPS-R (250, 500, 750, 1000, and 2000 µg/mL), were prepared in Dulbecco's modified Eagle's medium (DMEM) (LONZA, Verviers, Belgium) for human fibroblast (ATCC: CCL-186) cell lines. The culture media were supplemented with Fetal Calf Serum (FCS) (10% v/v) and 1% (w/v) Penicillin-streptomycin (Gibco, Rockville, MD, USA). The cell viabilities were subsequently assessed using a luminescence assay that was based on Adenosine triphosphate quantification (CellTiter-Glo (Promega, Madison, Wisconsin)). Cell lines passage 19 were cultured and incubated at 37 ˚C, in a 5 v/v% CO_2-humidified atmosphere. At cell confluency of 80%, the cells were retrieved and placed in triplicate in a white assay 96-well plate with 10^4/well density. 50 µL of the Scl and EPS-R samples were then used in the treatment of the human fibroblast cells after which, 50 µL of RealTime-Glo™ MT Cell Viability kit components, was added. Control cells were also cultured in a media in the absence of Scl and EPS. Cell viability was subsequently evaluated by monitoring Luminescence on a Microplate luminometer (Centro XS LB 960-Berthold) set at 0, 24, and 30 h, following the manufacturer's instructions.

***In vivo* wound healing experiments**

In vivo experiments were conducted to assess the wound healing effects of the extracted Scl and the EPS-R, using simulated wounds. 48 adult male Wistar rats (2 months old, weighing 200–220 g) were employed. The experiments were conducted in accordance with the National Institute of Health guidelines and the European Communities Council Directive (2010/63/EU) and approved by the Kermanshah University of Medical Sciences (IR.KUMS.REC.1400.247). Initially, the rats were divided into eight groups (Groups 1-8), with each group containing 6 rats. Group 1 was the negative control, which represented wounds without treatment, Group 2 was the positive control group, which represented wounds treated with commercial phenytoin cream 1%, while Groups 3, 4, and 5, denoted wounds treated with 1 mg/mL, 5 mg/mL, and 10 mg/mL of Scl solutions, respectively and Groups 6, 7 and 8, denoted wounds treated with EPS-R solutions at concentrations of 1, 5, and 10 mg/mL, respectively. Prior to simulating the wounds, the rat models were subjected to general anesthesia composed of Ketamine 5% (70 mg/kg) and Xylazine 2% (6 mg/kg). Administration of the anesthesia was achieved using an intraperitoneal injection (IP). The back hair of the rat models was shaved, and the bare skin was subsequently sterilized using 70% (v/v) ethanol (Ghalayani Esfahani et al. 2020) after which a circular full-thickness excision (diameter of 1 cm) was introduced with the bare skin. The wounds were then subjected to different treatments in accordance with the different rat groupings and subsequently evaluated to assess the percentage of wound closure (*WC%*) as follows;

$$WC\% = \left(1 - \frac{OP_w}{IP_w}\right) 100 \quad (3)$$

where OP_w denotes the open wound area, in m^2 IP_w denotes the initial wound area, in m^2.

Histopathological evaluations were also undertaken using the Hematoxylin and Eosin (H&E) and Masson's trichrome (MT) staining technique after 14 d of treatment. An IP injection of a mixture of ketamine/Xylazine (150/20 mg per kg) was used to euthanize the rats, after which the wound area was harvested. The harvested wound area was then prepared in buffered formalin (10%, pH: 7.4) for 48 h, blocked, sectioned, and stained using H&E and MT.

Statistical analysis

All data are presented as the mean ± standard derivation (SD). GraphPad Prism 9.0.0 (GraphPad Software, LLC, USA) was used for *in vitro* and *in vivo* data analysis as well as for graph production. Since the data (*WC*% and cell viability results) followed a non-parametric distribution, the two-way ANOVA test followed by Dunnett's multiple comparisons was used. When $p < 0.05$, statistical significance was found.

Results

EPSs production and characterization

The total yield of the Scl produced by *S. glucanicum* and the EPS yielded by *R. babjevae* (EPS-R) was 0.9 ± 0.07 g/L and 1.11 ± 0.4 g/L, respectively. Further assessment of the Scl via the phenol-sulphuric acid method showed that the EPS mainly contained carbohydrates (91.29 % ± 1.71%, weight basis). The residual portion of the Scl (8.71 ± 3.42 %) was attributed to ash and non-carbohydrate substituents in the Scl such as proteins, nucleic acids, sulfate, pyruvate, methyl, or acetyl groups (Delattre et al. 2016). Moreover, the phenol-sulphuric acid method showed that the water-soluble EPS-R (Mirzaei Seveiri et al. 2020) contained mainly carbohydrates (80.1 ± 1.23%, weight basis%), similar to a previous study (Mirzaei Seveiri et al. 2020) (Mirzaei Seveiri et al. 2020). The residual portion of the EPS-R (19.9 ± 2.46 %) was also attributed to ash and non-carbohydrate substituents in the EPS-R such as proteins, nucleic acids, sulfate, pyruvate, methyl, or acetyl groups (Delattre et al. 2016).

Fig. 1

The SEM image of the Scl and FT-IR spectrum of both EPSs are represented in Fig. 1. The extracted Scl showed irregular fibril (Fig. 1a). Fig. 1b, shows a broad peak at 3302.83 cm^{-1}, which is due to the stretching vibrations of O–H and indicates the presence of polymeric O–H compounds i.e. repetitive units of O-H

monomers (Okoro and Sun 2020). The sharp peak observed at 2929.40 cm^{-1} is due to the stretching vibrations of C–H indicating the presence of the CH_3 functional group (Vasanthakumari et al. 2015). The peaks observed at 1644.69 cm^{-1} and 1410.63 cm^{-1} can be attributed to C=O stretching and C–H bending vibrations of carboxylic and CH_3 or/and CH_2 functional groups, respectively (Shuhong et al. 2014; Okoro and Sun 2020). Sharp peaks at 1087.90 cm^{-1} and 644.31 cm^{-1} indicate the presence of C—O—C bonds and glycosidic linkages, respectively (Shuhong et al. 2014; Vasanthakumari et al. 2015).

In vitro biological activities

Antioxidant activity

The antioxidant activity of the extracted Scl, measured in terms of the DPPH• scavenging activity rate, shows a positive correlation with concentration such that higher concentrations of 0.5 mg/mL increased scavenging activities (Fig. 2a). Also, the free radicals (DPPH•, •OH, $O_2^{-\bullet}$) scavenging activities of the EPS-R were observed to be dose-dependent and higher than hyaluronic acid (molecular weight 1,000,000-1,250,000 Da) (Mirzaei Seveiri et al. 2020) (a biopolymer that may scavenge free radicals and is used in cosmetics) in the previous study (Mirzaei Seveiri et al. 2020).

Hemocompatibility

The hemocompatibility of both EPSs was investigated at different concentrations (1, 5, and 10 mg/mL) using anticoagulated human blood (Fig. 2b). For all tested concentrations of the EPSs, there was significantly less hemolysis (5-8%) compared to the positive control (distilled water), demonstrating that the EPSs did not induce significant hemolysis or damage to human RBCs. EPSs did not have any adverse effect on the rupturing of RBCs (Raveendran et al. 2013).

Cell viability assay

The outcome of the treatment of human dermal fibroblast (HDF) (ATCC: CCL-186) cell line with the extracted Scl is shown in Fig. 2c. No decrease in cell viability was observed after treatment of the HDF cell line with the Scl concentrations varying from 400 µg/mL to 1000 µg/mL. Indeed, Scl was shown to enhance the viability of HDF cells at a concentration of 600 µg/mL in comparison with the control group, demonstrating that the Scl from *S. glucanicum* DSM 2159 could promote the proliferation of HDF cells at this concentration. Also, Fig. 2d shows that the EPS-R was cytocompatible at all the tested concentrations (250-2000 µg/mL) when applied to the HDF cell line until 30 h of incubation.

Fig. 2

In vivo wound healing effects of scleroglucan and EPS from _R. babjevae_

The full-thickness wound model on the back of rats was applied to assess the wound healing potential of the extracted Scl and the EPS-R. The animals were treated with different concentrations of the Scl and EPS-R for 14 days and the healing process was monitored using *WC%* measurements during the treatment and histopathology observations (H&E and MT staining) at the end of the treatment (Fig. 3&4). Normal skin (without injury and treatment) was provided for comparison with the control groups and the test groups.

Fig. 3 & Fig. 4

When Scl was applied to the wound model, the highest *WC%* of 98 ± 0.82%, was obtained after treatment with the Scl 10 mg/mL which was statistically significant ($p < 0.05$), compared to the mean *WC%* of the negative control group of 84.33 ± 2.49%. The *WC%* of 98 ± 0.82% after treatment with Scl 10 mg/mL was comparable to the *WC%* recorded in the positive control group (98.33 ± 1.25%) (i.e., treatment with Phenytoin ointment of 1%).

The histopathological analysis using H&E and MT staining is presented in Fig. 3c. Also, Fig. 4 shows the *WC*% for the different test groups treated with the EPS-R, positive and negative controls, and the results of the histopathological evaluation of the wound healing potential of the EPS-R. Conclusively, Fig. 5 shows the relationship between *WC*% in controls and two test groups treated with the highest concentration of the samples (Scl/EPS-R 10 mg/mL) at different time intervals.

Fig. 5

H&E staining results presented in Fig. 3c and Fig. 4c show that in the negative control group, 14 days was inadequate to facilitate the full development of the epidermal layer with wound healing stagnating at the inflammatory phase as revealed by the infiltration of polymorphonuclear inflammatory cells (PMNs). The wound bed was also observed to be covered by crusty scabs (thick arrows in Fig. 3c & 4c) in these groups. Fig. 3c & 4c further indicate that after 14 days, partial epidermal layer development was evident in wounds treated with Scl/EPS-R at 1 mg/mL and 5 mg/mL doses.

Discussion

For the first time, in this study, the biological and wound healing performances of Scl and a new EPS from the yeast *R. babjevae*, were characterized that could be a promising biocomponent for wound healing acceleration. The total yield of the Scl produced by *S. glucanicum (*0.9 ± 0.07 g/L) was not comparable to the Scl yields of 7.14 – 42 g/L reported in the literature (Selbmann et al. 2002; Zeng et al. 2021). This lower yield can be attributed to the differences in fungal strains employed in the EPS production. Furthermore, the lower yield of the Scl in the present study also highlights the need to undergo further optimization studies to enhance the Scl

yield from the strain used in this study. Additionally, the yield of the EPS-R of 1.11 ± 0.4 g/L was determined to be comparable to the yield of 1.6 ± 0.2 g/L reported in our previous study (Mirzaei Seveiri et al. 2020).

The microstructure of the Scl (Fig. 1a) produced by *S. glucanicum* DSM 2159 was similar to the morphology of Scl from *Athelia* (*Sclerotium*) *rolfsii* TEMG reported by Elsehemy et al. (Elsehemy et al. 2020a). Moreover, based on the earlier report (Mirzaei Seveiri et al. 2020), the EPS-R micrographs (Fig. 1b) have displayed a porous, three-dimensional structure, with numerous cracks visible in their microstructure.

The peaks detected from the FT-IR spectrum (Fig. 1c), showed that the Scl produced by *S. glucanicum* DSM 2159 has an identical FT-IR spectrum to the previously reported spectra of Scl from *S. rolfsii* ATCC 201126 and the commercial Scl (LSCL) (Valdez et al. 2019) and also the commercial Scl used in this study. In addition, the FT-IR spectrum from *R. babjevae* (Fig. 1c), is similar to the previously described spectra in the literature (Mirzaei Seveiri et al. 2020).

The results of DPPH• assay demonstrated that the Scl enforces a dose-dependent antioxidant activity. This dose-dependent antioxidant activity by the Scl produced by *S. glucanicum* DSM 2159 was anticipated since a similar observation was reported in the work by Elsehemy et al. when the scavenging activity of DPPH• by Scl from *Athelia rolfsii* TEMG was increased from ~17.5 % to ~50% as the concentration increased from 50 to 800 µg/mL (Elsehemy et al. 2020a). Moreover, there are several reports regarding the radical scavenging activities of microbial EPSs. For instance, *Leuconostoc mesenteroides* Shen Nong's (SN)-8 produced a new EPS. The structural analysis of EPS revealed that it belonged to the polysaccharide class and was primarily made of glucan. It also contained a small number of mannose residues, which were discovered to be linked by α-1,6 glycosidic linkages. Additionally, the findings showed that EPS had a notable ability to partially scavenge free radicals and that this anti-oxidant capability was concentration-dependent (Wu et al. 2021). In another study, an EPS was found in a fungal strain called *Lachnum* YM262. The EPS had a mannose to galactose molar ratio of 20.6:1 and exhibited a sharp increase in scavenging activity at the samples' concentration range (0–3 mg/mL). The EPS' DPPH radical scavenging rate was 78.3% at a concentration of 3.0 mg/mL (Chen et al. 2017). According to Xia et al., EPS (0.2-1 mg/mL) isolated from *Cupriavidus pauculus* 1490 obtained its maximal DPPH radical scavenging activity at 0.8 mg/mL for EPS (69%) and ascorbic acid (97.9%), respectively. The primary monosaccharides found in EPS were mannose, glucuronic acid, glucose, and xylose. (Xia et al. 2022). Thus, these findings are in agreement with Liang et al. who claimed that some microbial polysaccharides have antioxidant properties and can be exploited to make immune modulators (Liang et al. 2016; Ho Do et al. 2021)

and EPSs having antioxidant activities may be a suitable candidate to be used as a biomaterial in wound healing and skin tissue regeneration (Sun et al. 2020; Comino-Sanz et al. 2021).

Sun et al. hypothesized that the presence of functional groups such as -O-, C=O, and -OH in the EPS's structure may be responsible for its capacity to scavenge free radicals (Sun et al. 2015a). It is generally accepted that the aforementioned functional groups can directly bind to free radicals to produce stable radicals as well as donate electrons or hydrogen ions to reduce the free radicals (Sun et al. 2015a; Liang et al. 2016; Wang et al. 2016). The presence of the abovementioned functional groups in our EPS structures was confirmed via the FT-IR spectrum (Fig. 1).

The antioxidant activities of EPSs are not dependent on a single factor but rather are the consequence of the interaction of several factors including the ratios of monosaccharide, molecular weight, and glycosidic branching (Chen et al. 2017; Zhu et al. 2018). Nevertheless, the underlying mechanism responsible for the antioxidant activity of the EPSs has not been fully illustrated (Kurečič et al. 2018).

There are a few reports in the literature regarding the hemocompatibility evaluation of microbial EPS. For example, Mauran, a highly polyanionic sulfated EPS from moderately halophilic bacterium; *Halomonas maura*, was hemocompatible, when the highest concentration (1 mg/mL) was investigated demonstrating only 1.059 ± 0.26% of hemolysis on human RBCs (Raveendran et al. 2013). Also, MBF-15 EPS obtained from *Paenibacillus jamilae* was hemocompatible (using mouse RBCs), when the maximum hemolysis percentage detected was 0.76 ± 0.14% (Zhong et al. 2018).

The data of cell viability experiments are consistent with previous findings of cell toxicity for microbial EPSs in the literature. For example, Scl from *Athelia rolfsii* TEMG showed no cytotoxic effect against normal human fibroblast (WI 38) up to 4000 µg/mL assessed by MTT assay (Elsehemy et al. 2020a). On the other hand, the IC_{50} of the Scl toward WI 38, human liver carcinoma cells (HepG2), and human prostate cancer (PC3) cell lines was 5096.83 µg/mL, 5885.8 µg/mL, and 4803.90 µg/mL, respectively (Elsehemy et al. 2020a). Thus, the results revealed no significant changes between WI 38 cells, which represent normal cell lines, and HepG2 and PC3, which represent cancer cell lines. Furthermore, Liu et al. (Liu et al. 2021a), Wang et al. (Wang et al. 2018), and Uhliariková et al. (Uhliariková et al. 2020), found that the EPS from *Phomopsis liquidambari* NJUSTb1, *Lactobacillus plantarum* JLK0142, and cyanobacterium *Nostoc* sp., respectively, had no toxic effects on macrophage cell line (RAW 264.7) and promoted its proliferation. Moreover, the EPSs from *Rhodotorula mucilaginosa* sp. GUMS16 (Hamidi et al. 2020), *Weissella cibaria* (Vasanthakumari et al. 2015), and

Nitratireductor sp. PRIM-31 (Priyanka et al. 2016) was reported to be biocompatible with human fibroblast cell lines. Also, it was shown that the EPS-R was biocompatible with MDCK cell line (Mirzaei Seveiri et al. 2020).

The animal studies showed dose-dependent wound healing effects after treatment with both EPSs. Notably, a dose-dependent *WC*% was observed since a positive correlation existed between increasing EPSs concentrations and increasing *WC*%. Interestingly, for treatments using Scl (10 mg/mL) and EPS-R (10 mg/mL), *WC*% of 98 ± 0.82% and 99 ± 0.82% were determined, respectively, and were comparable to the *WC*% (98.33 ± 1.25%), achieved after treatment with commercial phenytoin 1% cream after 14 days. Thus, a dose-dependent wound healing capacity of the EPSs was determined and there was no significant difference between the two EPSs at the highest concentration (10 mg/mL) regarding their effects on *WC%*.

The best wound healing outcome between the test groups was obtained after treatment with Scl/EPS-R 10 mg/mL, which induced partially complete epidermal layer formation. Moreover, collagen fiber production and distribution were stained using MT staining during the healing process. As shown in Fig. 3c & 4c (right images with thick arrows), the collagen fibers are disordered and discontinuous in the negative control group and treatment using Scl/EPS-R 1 and 5 mg/mL. Increasing the concentration of Scl/EPS-R to 10 mg/mL induced more ordered and continuous collagen fiber synthesis (arrowheads). The Scl/EPS-R 10 mg/mL group had collagen fiber formation and maturation, as seen in Fig. 3c & 4c. Moreover, collagen fiber production and distribution were stained using MT staining during the healing process.

Microbial EPSs such as β-glucans, bacterial cellulose, and hyaluronic acid have wound healing applications due to their antioxidant, antimicrobial, and proliferative effects (Trabelsi et al. 2017; Mohd Nadzir et al. 2021). For instance, an EPS from *Polaribacter* sp. SM1127 was used to promote wound healing in rat skin (Sun et al. 2015b). Scratch wound assay demonstrated that the EPS could promote HDF cells migration. Also, the capacity of SM1127 EPS to enhance skin wound healing was demonstrated in the full-thickness cutaneous wound experiment using Sprague-Dawley (SD) rats. The EPS boosted the wound healing rate and stimulated tissue repair, which was observed by microscopy and histologic investigation (Sun et al. 2020).

Clinically, β-glucans have been used as a wound dressing to promote wound healing (Williams 1999; Majtan and Jesenak 2018). Macrophages, keratinocytes, and fibroblasts are the main target cells of β-glucans during wound healing. β-glucans increase macrophage infiltration, which promotes tissue granulation, collagen deposition, and reepithelialization, which aids wound healing. Nissola et al. examined the wound healing ability of a hydrogel containing Lasiodiplodan (a linear (1,6) fungal β-glucan) on the Wistar rats. Cell re-epithelialization and proliferation were enhanced by the hydrogel, as well as collagen fiber synthesis (Nissola et

al. 2021). Cheng et al. assessed the wound healing efficacy of hot aqueous extract of *Ganoderma lucidumin* (10% w/w) having β-glucan in diabetic rats and observed that the *WC%* (97%) was higher than the positive control group (70%) (treated with Intrasite gel) after 12 days. The results also showed high antioxidant activity in the serum of rats and lower lipid damage and oxidative protein products under treatment with the extract compared to the controls (Cheng et al. 2013). Additionally, Bae et al. evaluated the wound healing efficacy of EPS isolated from *Phellinus gilvus* (Schw.), and observed enhanced wound healing in normal and diabetic rats (Bae et al. 2005a; Bae et al. 2005b). These studies proposed that the wound healing mechanism under treatment with the EPSs containing glucan may involve the modulation of the macrophages and fibroblasts migration and an increased rate of type I and III collagen biosynthesis due to their antioxidant and proliferative effects.

Mannans can also increase blood vessel regeneration and stimulate macrophage activities, therefore it may be developed as wound-healing materials (Liu et al. 2021b). For instance, Jiang et al. determined that the mannan EPS produced from *Phellinus pini* displayed elevated macrophage-activating ability for enhanced phagocytosis *via* nitric oxide production, tumor necrosis factor, and reactive oxygen species (Jiang et al. 2016). Also, in our recent work, the EPS from *Papiliotrema terrestris* PT22AV was used to evaluate the wound healing effects in rats. Like the Scl and EPS-R, the EPS from *P. terrestris* PT22AV presented a dose-dependent wound healing effect using an *in vivo* full-thickness wound model (Hamidi et al. 2022b).

Even though β-glucan and mannan have been used in various fields, there are still several challenges to be resolved. The purity, molecular weight, and spatial structure of β-glucans and mannans produced by various extraction, separation, and purification procedures were all varied, resulting in diverse biological activity (Liu et al. 2021b). As a result, more tests were needed to investigate the effect of the structure-activity and dose-activity relationships on the biological activities of EPSs, including the two fungal EPSs used in this study (Liu et al. 2021b).

Overall, in this study, two fungal EPSs produced by *S. glucanicum* and *R. babjevae* were extracted and partially characterized. The biological properties of the EPSs were examined via *in vitro* and *in vivo* studies. The EPSs were determined to be hemocompatible and cytocompatible toward human fibroblast cell lines. Furthermore, *in vivo* tests using the full thickness wound models showed that both EPSs facilitated wound healing at the concentration of 10 mg/mL. These findings demonstrated that the EPSs from *S. glucanicum* and *R. babjevae* constitute a promising biopolymer for wound healing and may be utilized in the manufacture of wound dressings.

Acknowledgements

M.H would like to acknowledge the postdoctoral fellowship provided by the European Program IF@ULB-MARIE SKŁODOWSKA-CURIE Cofund Action (European Horizon 2020). This project has received funding from the European Union's Horizon 2020 research and innovation program under the Marie Skłodowska-Curie grant agreement No. 801505. The graphical abstract was prepared using Biorender.com. Also, we must thank Dr. Mahta Mirzaei for her kind help in cell viability assays. The CARAMAT platform at the ULB also received acknowledgement from the authors for its help with SEM investigation.

References

Ai, A., Behforouz, A., Ehterami, A., Sadeghvaziri, N., Jalali, S., Farzamfar, S., et al. (2019) Sciatic nerve regeneration with collagen type I hydrogel containing chitosan nanoparticle loaded by insulin. International Journal of Polymeric Materials and Polymeric Biomaterials 68(18): 1133-1141.

Apostolopoulos, V. and McKenzie, I.F. (2001) Role of the mannose receptor in the immune response. Curr Mol Med 1(4): 469-474.

Bae, J.-s., Jang, K.-h., Park, S.-c. and Jin, H.K. (2005a) Promotion of dermal wound healing by polysaccharides isolated from Phellinus gilvus in rats. Journal of veterinary medical science 67(1): 111-114.

Bae, J.S., Jang, K.H. and Jin, H.K. (2005b) Polysaccharides isolated from Phellinus gilvus enhances dermal wound healing in streptozotocin-induced diabetic rats. Journal of Veterinary Science 6(2): 161-164.

Chatterjee, S., Mukhopadhyay, S.K., Gauri, S.S. and Dey, S. (2018) Sphingobactan, a new α-mannan exopolysaccharide from Arctic Sphingobacterium sp. IITKGP-BTPF3 capable of biological response modification. Int Immunopharmacol 60(84-95.

Chen, T., Xu, P., Zong, S., Wang, Y., Su, N. and Ye, M. (2017) Purification, structural features, antioxidant and moisture-preserving activities of an exopolysaccharide from Lachnum YM262. Bioorganic & Medicinal Chemistry Letters 27(5): 1225-1232.

Cheng, P.-G., Phan, C.-W., Sabaratnam, V., Abdullah, N., Abdulla, M.A. and Kuppusamy, U.R. (2013) Polysaccharides-rich extract of Ganoderma lucidum (MA Curtis: Fr.) P. Karst accelerates wound healing in streptozotocin-induced diabetic rats. Evid Based Complement Alternat Med 2013(

Comino-Sanz, I.M., López-Franco, M.D., Castro, B. and Pancorbo-Hidalgo, P.L. (2021) The Role of Antioxidants on Wound Healing: A Review of the Current Evidence. Journal of Clinical Medicine 10(16): 3558.

de Torre, M.P., Cavero, R.Y., Calvo, M.I. and Vizmanos, J.L. (2019) A simple and a reliable method to quantify antioxidant activity in vivo. Antioxidants 8(5): 142.

Decho, A.W. and Gutierrez, T. (2017) Microbial Extracellular Polymeric Substances (EPSs) in Ocean Systems 8(922).

Delattre, C., Pierre, G., Laroche, C. and Michaud, P. (2016) Production, extraction and characterization of microalgal and cyanobacterial exopolysaccharides. Biotechnology Advances 34(7): 1159-1179.

Dubois, M., Gilles, K.A., Hamilton, J.K., Rebers, P.t. and Smith, F. (1956) Colorimetric method for determination of sugars and related substances. Anal Chem 28(3): 350-356.

El-Ghonemy, D.H. (2021) Antioxidant and antimicrobial activities of exopolysaccharides produced by a novel *Aspergillus* sp. DHE6 under optimized submerged fermentation conditions. Biocatalysis and Agricultural Biotechnology 36(102150.

Elsehemy, I.A., Noor El Deen, A.M., Awad, H.M., Kalaba, M.H., Moghannem, S.A., Tolba, I.H., et al. (2020a) Structural, physical characteristics and biological activities assessment of scleroglucan from a local strain Athelia rolfsii TEMG. Int J Biol Macromol 163(1196-1207.

Elsehemy, I.A., Noor El Deen, A.M., Awad, H.M., Kalaba, M.H., Moghannem, S.A., Tolba, I.H., et al. (2020b) Structural, physical characteristics and biological activities assessment of scleroglucan from a local strain Athelia rolfsii TEMG. International Journal of Biological Macromolecules 163(1196-1207.

Geller, A. and Yan, J. (2020) Could the induction of trained immunity by β-glucan serve as a defense against COVID-19? Front Immunol 11(1782.

Ghada, S.I., Manal, G.M., Mohsen, M. and Eman, A.G. (2012) Production and biological evaluation of exopolysaccharide from isolated Rhodotorula glutinins. Australian Journal of Basic and Applied Sciences 6(3): 401-408.

Ghalayani Esfahani, A., Altomare, L., Bonetti, L., Nejaddehbashi, F., Boccafoschi, F., Chiesa, R., et al. (2020) Micro-Structured Patches for Dermal Regeneration Obtained via Electrophoretic Replica Deposition. Applied Sciences 10(14): 5010.

Hamidi, Okoro, O.V., Milan, P.B., Khalili, M.R., Samadian, H., Nie, L., et al. (2022a) Fungal exopolysaccharides: Properties, sources, modifications, and biomedical applications. Carbohydr Polym119152.

Hamidi, M., Gholipour, A.R., Delattre, C., Sesdighi, F., Mirzaei Seveiri, R., Pasdaran, A., et al. (2020) Production, characterization and biological activities of exopolysaccharides from a new cold-adapted yeast: *Rhodotorula mucilaginosa* sp. GUMS16. Int J Biol Macromol 151(268-277.

Hamidi, M., Okoro, O.V., Ianiri, G., Jafari, H., Rashidi, K., Ghasemi, S., et al. (2022b) Exopolysaccharide from the yeast *Papiliotrema terrestris* PT22AV for skin wound healing. Journal of Advanced Research.

Han, B., Baruah, K., Cox, E., Vanrompay, D. and Bossier, P. (2020) Structure-functional activity relationship of β-glucans from the perspective of immunomodulation: a mini-review. Front Immunol 11(658.

Ho Do, M., Seo, Y.S. and Park, H.-Y. (2021) Polysaccharides: bowel health and gut microbiota. Critical reviews in food science and nutrition 61(7): 1212-1224.

Jaroszuk-Ściseł, J., Nowak, A., Komaniecka, I., Choma, A., Jarosz-Wilkołazka, A., Osińska-Jaroszuk, M., et al. (2020) Differences in Production, Composition, and Antioxidant Activities of Exopolymeric Substances (EPS) Obtained from Cultures of Endophytic Fusarium culmorum Strains with Different Effects on Cereals. Molecules (Basel, Switzerland) 25(3): 616.

Jiang, P., Yuan, L., Huang, G., Wang, X., Li, X., Jiao, L., et al. (2016) Structural properities and immunoenhancement of an exopolysaccharide produced by *Phellinus pini*. International journal of biological macromolecules 93(566-571.

Keshavarz, S., Azizian, R., Malakootikhah, J., Fathizadeh, H. and Hamidi, M. (2022) Microbial Exopolysaccharides in Additive Manufacturing. In *Encyclopedia of Green Materials* eds. Baskar, C., Ramakrishna, S. and Daniela La Rosa, A. pp.1-11. Singapore: Springer Nature Singapore.

Kurečič, M., Maver, T., Virant, N., Ojstršek, A., Gradišnik, L., Hribernik, S., et al. (2018) A multifunctional electrospun and dual nano-carrier biobased system for simultaneous detection of pH in the wound bed and controlled release of benzocaine. Cellulose 25(12): 7277-7297.

Kwon, A.-H., Qiu, Z., Hashimoto, M., Yamamoto, K. and Kimura, T. (2009) Effects of medicinal mushroom (Sparassis crispa) on wound healing in streptozotocin-induced diabetic rats. The American Journal of Surgery 197(4): 503-509.

Liang, T.-W., Tseng, S.-C. and Wang, S.-L. (2016) Production and characterization of antioxidant properties of exopolysaccharide (s) from Peanibacillus mucilaginosus TKU032. Marine drugs 14(2): 40.

Liu, J.-S., Zeng, Y.-X., Bi, S.-Y., Zhou, J.-W., Cheng, R., Li, J., et al. (2021a) Characterization and chemical modification of PLN-1, an exopolysaccharide from *Phomopsis liquidambari* NJUSTb1. Carbohydr Polym 253(117197.

Liu, Y., Wu, Q., Wu, X., Algharib, S.A., Gong, F., Hu, J., et al. (2021b) Structure, preparation, modification, and bioactivities of β-glucan and mannan from yeast cell wall: A review. International Journal of Biological Macromolecules.

Mahapatra, S. and Banerjee, D. (2013) Fungal exopolysaccharide: production, composition and applications. Microbiology insights 6(MBI. S10957.

Majtan, J. and Jesenak, M. (2018) β-Glucans: multi-functional modulator of wound healing. Molecules 23(4): 806.

Masoud Hamidi, Rasool Mirzaei, Cédric Delattre, Korosh Khanaki, Guillaume Pierre, Christine Gardarin, et al. (2018) Characterization of a new exopolysaccharide produced by *Halorubrum* sp. TBZ112 and evaluation of its anti-proliferative effect on gastric cancer cells. 3 Biotech.

Mirzaei Seveiri, R., Hamidi, M., Delattre, C., Sedighian, H., Pierre, G., Rahmani, B., et al. (2020) Characterization and Prospective Applications of the Exopolysaccharides Produced by *Rhodosporidium babjevae*. Adv Pharm Bull 10(2): 254-263.

Mohd Nadzir, M., Nurhayati, R.W., Idris, F.N. and Nguyen, M.H. (2021) Biomedical Applications of Bacterial Exopolysaccharides: A Review. Polymers 13(4): 530.

Nissola, C., Marchioro, M.L.K., de Souza Leite Mello, E.V., Guidi, A.C., de Medeiros, D.C., da Silva, C.G., et al. (2021) Hydrogel containing (1 → 6)-β-D-glucan (lasiodiplodan) effectively promotes dermal wound healing. International Journal of Biological Macromolecules 183(316-330.

Okoro, O.V., Gholipour, A.R., Sedighi, F., Shavandi, A. and Hamidi, M. (2021) Optimization of Exopolysaccharide (EPS) Production by *Rhodotorula mucilaginosa* sp. GUMS16. ChemEngineering 5(3): 39.

Okoro, O.V. and Sun, Z. (2020) The characterisation of biochar and biocrude products of the hydrothermal liquefaction of raw digestate biomass. Biomass Conversion and Biorefinery.

Pirhanov, A., Bridges, C.M., Goodwin, R.A., Guo, Y.-S., Furrer, J., Shor, L.M., et al. (2021) Optogenetics in Sinorhizobium meliloti enables spatial control of exopolysaccharide production and biofilm structure. ACS Synthetic Biology 10(2): 345-356.

Pretus, H., Ensley, H., McNamee, R., Jones, E., Browder, I.W. and Williams, D. (1991) Isolation, physicochemical characterization and preclinical efficacy evaluation of soluble scleroglucan. Journal of Pharmacology and Experimental Therapeutics 257(1): 500-510.

Priyanka, P., Arun, A., Ashwini, P. and Rekha, P. (2016) Functional and cell proliferative properties of an exopolysaccharide produced by Nitratireductor sp. PRIM-31. International journal of biological macromolecules 85(400-404.

Rana, S. and Upadhyay, L.S.B. (2020) Microbial exopolysaccharides: Synthesis pathways, types and their commercial applications. International Journal of Biological Macromolecules 157(577-583.

٥٥٢ Raveendran, S., Palaninathan, V., Chauhan, N., Sakamoto, Y., Yoshida, Y., Maekawa, T., et al. (2013) In vitro
٥٥٣ evaluation of antioxidant defense mechanism and hemocompatibility of mauran. Carbohydr Polym 98(1): 108-
٥٥٤ 115.
٥٥٥ Sajna, K.V., Sharma, S. and Nadda, A.K. (2021) Microbial Exopolysaccharides: An Introduction. In *Microbial*
٥٥٦ *Exopolysaccharides as Novel and Significant Biomaterials* ed. al., A.K.N.e. Switzerland: Springer.
٥٥٧ Sathishkumar, R., Kannan, R., Jinendiran, S., Sivakumar, N., Selvakumar, G. and Shyamkumar, R. (2021)
٥٥٨ Production and characterization of exopolysaccharide from the sponge-associated Bacillus subtilis MKU
٥٥٩ SERB2 and its in-vitro biological properties. International Journal of Biological Macromolecules 166(1471-
٥٦٠ 1479.
٥٦١ Selbmann, L., Crognale, S. and Petruccioli, M. (2002) Exopolysaccharide production from Sclerotium
٥٦٢ glucanicum NRRL 3006 and Botryosphaeria rhodina DABAC-P82 on raw and hydrolysed starchy materials.
٥٦٣ Lett Appl Microbiol 34(1): 51-55.
٥٦٤ Shuhong, Y., Meiping, Z., Hong, Y., Han, W., Shan, X., Yan, L., et al. (2014) Biosorption of Cu2+, Pb2+ and
٥٦٥ Cr6+ by a novel exopolysaccharide from *Arthrobacter* ps-5. Carbohydr Polym 101(50-56.
٥٦٦ Sitepu, I.R., Sestric, R., Ignatia, L., Levin, D., German, J.B., Gillies, L.A., et al. (2013) Manipulation of culture
٥٦٧ conditions alters lipid content and fatty acid profiles of a wide variety of known and new oleaginous yeast
٥٦٨ species. Bioresource Technology 144(360-369.
٥٦٩ Sun, M.-L., Zhao, F., Chen, X.-L., Zhang, X.-Y., Zhang, Y.-Z., Song, X.-Y., et al. (2020) Promotion of Wound
٥٧٠ Healing and Prevention of Frostbite Injury in Rat Skin by Exopolysaccharide from the Arctic Marine Bacterium
٥٧١ Polaribacter sp. SM1127. Marine Drugs 18(1): 48.
٥٧٢ Sun, M.-L., Zhao, F., Shi, M., Zhang, X.-Y., Zhou, B.-C., Zhang, Y.-Z., et al. (2015a) Characterization and
٥٧٣ biotechnological potential analysis of a new exopolysaccharide from the Arctic marine bacterium Polaribacter
٥٧٤ sp. SM1127. Sci Rep 5(1): 1-12.
٥٧٥ Sun, M.-L., Zhao, F., Shi, M., Zhang, X.-Y., Zhou, B.-C., Zhang, Y.-Z., et al. (2015b) Characterization and
٥٧٦ Biotechnological Potential Analysis of a New Exopolysaccharide from the Arctic Marine Bacterium
٥٧٧ Polaribacter sp. SM1127. Sci Rep 5(1): 18435.
٥٧٨ Trabelsi, I., Ktari, N., Slima, S.B., Triki, M., Bardaa, S., Mnif, H., et al. (2017) Evaluation of dermal wound
٥٧٩ healing activity and in vitro antibacterial and antioxidant activities of a new exopolysaccharide produced by
٥٨٠ *Lactobacillus* sp. Ca_6. International journal of biological macromolecules 103(194-201.

٥٨١ Uhliariková, I., Šutovská, M., Barboríková, J., Molitorisová, M., Kim, H.J., Park, Y.I., et al. (2020) Structural
٥٨٢ characteristics and biological effects of exopolysaccharide produced by cyanobacterium *Nostoc* sp. International
٥٨٣ Journal of Biological Macromolecules 160(364-371.
٥٨٤ Valdez, A.L., Babot, J.D., Schmid, J., Delgado, O.D. and Fariña, J.I. (2019) Scleroglucan production by
٥٨٥ Sclerotium rolfsii ATCC 201126 from amylaceous and sugarcane molasses-based media: Promising insights for
٥٨٦ sustainable and ecofriendly scaling-up. Journal of Polymers and the Environment 27(12): 2804-2818.
٥٨٧ Vasanthakumari, D.S., Harikumar, S., Beena, D.J., Pandey, A. and Nampoothiri, K.M. (2015) Physicochemical
٥٨٨ characterization of an exopolysaccharide produced by a newly isolated Weissella cibaria. Applied biochemistry
٥٨٩ and biotechnology 176(2): 440-453.
٥٩٠ Viñarta, S.C., Delgado, O.D., Figueroa, L.I. and Fariña, J.I. (2013) Effects of thermal, alkaline and ultrasonic
٥٩١ treatments on scleroglucan stability and flow behavior. Carbohydr Polym 94(1): 496-504.
٥٩٢ Wang, J., Hu, S., Nie, S., Yu, Q. and Xie, M. (2016) Reviews on mechanisms of in vitro antioxidant activity of
٥٩٣ polysaccharides. Oxid Med Cell Longev 2016(
٥٩٤ Wang, J., Wu, T., Fang, X., Min, W. and Yang, Z. (2018) Characterization and immunomodulatory activity of
٥٩٥ an exopolysaccharide produced by *Lactobacillus plantarum* JLK0142 isolated from fermented dairy tofu.
٥٩٦ International journal of biological macromolecules 115(985-993.
٥٩٧ Williams, C. (1999) An investigation of the benefits of Aquacel Hydrofibre wound dressing. British Journal of
٥٩٨ Nursing 8(10): 676-680.
٥٩٩ Wu, J., Yan, D., Liu, Y., Luo, X., Li, Y., Cao, C., et al. (2021) Purification, structural characteristics, and
٦٠٠ biological activities of exopolysaccharide isolated from leuconostoc mesenteroides SN-8. Front Microbiol
٦٠١ 12(644226.
٦٠٢ Xia, M., Zhang, S., Shen, L., Yu, R., Liu, Y., Li, J., et al. (2022) Optimization and Characterization of an
٦٠٣ Antioxidant Exopolysaccharide Produced by Cupriavidus pauculus 1490. Journal of Polymers and the
٦٠٤ Environment 30(5): 2077-2086.
٦٠٥ Zeng, W., Wang, J., Shan, X., Yu, S. and Zhou, J. (2021) Efficient Production of Scleroglucan by Sclerotium
٦٠٦ rolfsii and Insights Into Molecular Weight Modification by High-Pressure Homogenization. Frontiers in
٦٠٧ bioengineering and biotechnology799.
٦٠٨ Zhong, C., Cao, G., Rong, K., Xia, Z., Peng, T., Chen, H., et al. (2018) Characterization of a microbial
٦٠٩ polysaccharide-based bioflocculant and its anti-inflammatory and pro-coagulant activity. Colloids Surf B
٦١٠ Biointerfaces 161(636-644.

Zhu, Y., Wang, C., Jia, S., Wang, B., Zhou, K., Chen, S., et al. (2018) Purification, characterization and antioxidant activity of the exopolysaccharide from Weissella cibaria SJ14 isolated from Sichuan paocai. International journal of biological macromolecules 115(820-828.

Statements & Declarations

Funding

This project has received funding from the European Union's Horizon 2020 research and innovation program under the Marie Skłodowska-Curie grant agreement No. 801505.

Competing interests

The authors declare that they have no known competing financial interests or personal relationships that could have appeared to influence the work reported in this paper.

Author contributions

MH: Conceptualization, Methodology, Formal analysis, Investigation, Validation, Writing-original draft, Writing-review & editing. **OVO**: Conceptualization, Investigation, Validation, Formal analysis, Writing-original draft, Writing-review & editing. **KR:** Investigation, Writing-review & editing. **MSS**: Investigation, Writing-review & editing. **RMS:** Investigation, Writing-review & editing. **HS:** Investigation, Supervision, Validation, Writing-review & editing. **AS:** Conceptualization, Validation, Resources, Supervision, Writing-review & editing, Visualization, Project administration, Funding acquisition.

Data availability

The datasets generated during and/or analyzed during the current study are available from the corresponding author on reasonable request.

Ethics approval and consent to participate

The animal experiments were conducted in accordance with the National Institute of Health guidelines and the European Communities Council Directive (2010/63/EU) and approved by Kermanshah University of Medical Sciences (IR.KUMS.REC.1400.247).

Consent to publish

Not applicable

Legends to illustrations

Fig. 1. a) SEM images showing the surface morphology of the scleroglucan produced by *S. glucanicum* DSM 2159 at ×900 and ×2000, magnifications. **b)** SEM images showing the surface morphology of the EPS from *R. babjevae* (EPS-R) at ×15000 and ×50000, magnifications. **c)** FT-IR spectrum of the commercial scleroglucan (commercial Scl), extracted scleroglucan from *S. glucanicum* DSM 2159 (Scl), and the EPS from *R. babjevae* (EPS-R).

Fig. 2. a) The DPPH radical scavenging activity (capacities) of the scleroglucan from *S. glucanicum* DSM 2159 with ascorbic acid as the positive control. **b)** Hemocompatibility assay of the scleroglucan from *S. glucanicum* DSM 2159 and the EPS from *R. babjevae* on human red blood cells. The results are expressed as hemolysis percentage in relation to the positive control (distilled water). The values are the means of 3 independent experiments performed in triplicate ± S.D. (*$p \leq 0.05$) versus the positive control group. RLU-RealTime-Glo™ cell viability assay of **c)** the scleroglucan from *S. glucanicum* DSM 2159 and **d)** the EPS from *R. babjevae* on human fibroblast cell (ATCC: CCL-186) line after 24h and 30h of incubation. Each value is expressed as mean ± SEM (n = 3) (*$p < 0.05$) versus control group (without EPSs).

Fig. 3. a) Contraction of excisional wounds in rats treated with three different concentrations of the scleroglucan (Scl) from *S. glucanicum* DSM 2159, sterile distilled water (as the negative control group) and Phenytoin 1% cream (as the positive control group). **b)** Percentage wound closure in controls and treated groups at different time intervals. Results are expressed as percentage wound closure and are the mean ± SD of three independent experiments. Data were analyzed using a two-way ANOVA test (*$p < 0.05$). **c)** Microscopic images of Hematoxylin and Eosin (left) and Masson's trichrome (right) -stained tissues after 14-days post-surgery in three different magnifications after 14-days post-surgery in three different magnifications. *Thick arrow in H&E: Crusty scab, Thick arrow in MT: disordered collagen fibers, Arrowhead: Ordered connective tissue, Thin arrow: polymorphonuclear inflammatory cells, E: Epidermis layer, F: Hair follicle.*

Fig. 4. a) Contraction of excisional wounds in rats treated with three different concentrations of the EPS from *R. babjevae*, sterile distilled water (as negative control group) and Phenytoin 1% cream (as positive control group). **b)** The relationship between percentage wound closure in controls and treated groups at different time intervals. Results are expressed as percentage wound closure and are the mean ± SD of three independent experiments. Data were analyzed using a two-way ANOVA test (*$p < 0.05$). **c)** Microscopic images of Hematoxylin and Eosin (left) and Masson's trichrome (right) -stained tissues after 14-days post-surgery in three different magnifications after 14-days post-surgery in three different magnifications. *Thick arrow in H&E: Crusty scab,*

Thick arrow in MT: disordered collagen fibers, Arrowhead: Ordered connective tissue, Thin arrow: polymorphonuclear inflammatory cells, E: Epidermis layer, F: Hair follicle, S: sebaceous glands.

Fig. 5. The relationship between percentage wound closure percent in controls and Scl/EPS 10 mg/mL groups at different time intervals. Results are expressed as wound closure % and are the mean ± SD of three independent experiments. Data were analyzed using a two-way ANOVA test (*$p < 0.05$).

a)

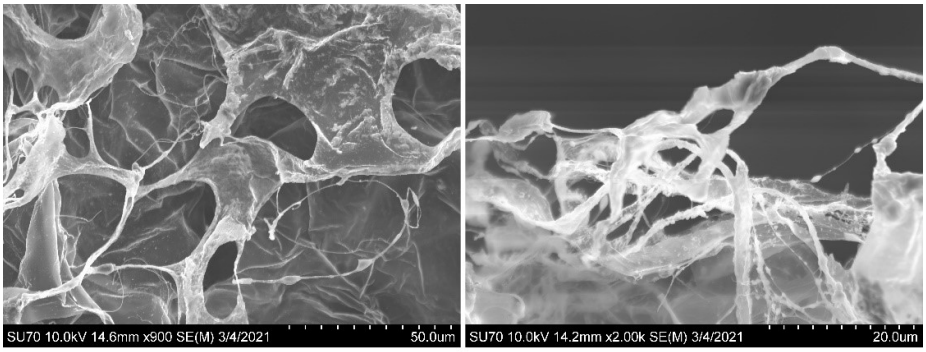
SU70 10.0kV 14.6mm x900 SE(M) 3/4/2021
50.0um
SU70 10.0kV 14.2mm x2.00k SE(M) 3/4/2021
20.0um

b)

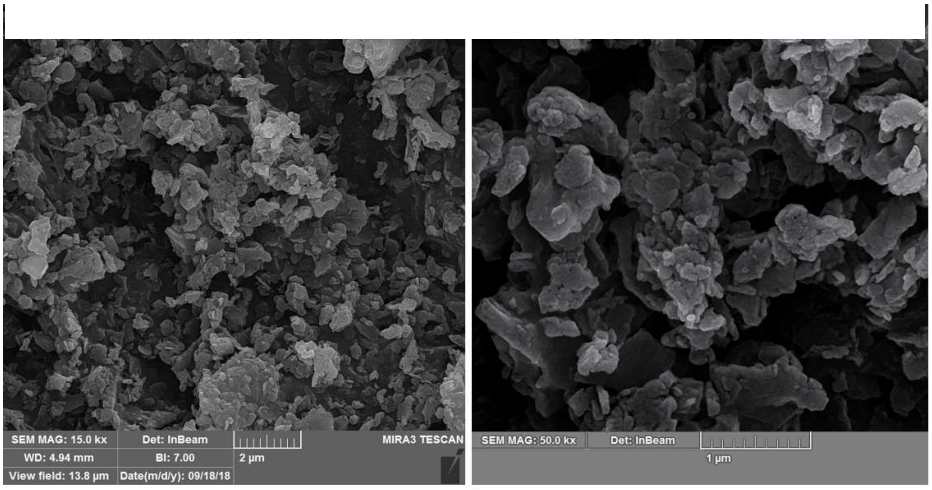
SEM MAG: 15.0 kx
Det: InBeam
MIRA3 TESCAN
WD: 4.94 mm
BI: 7.00
2 µm
View field: 13.8 µm
Date(m/d/y): 09/18/18
SEM MAG: 50.0 kx
Det: InBeam
1 µm

c)

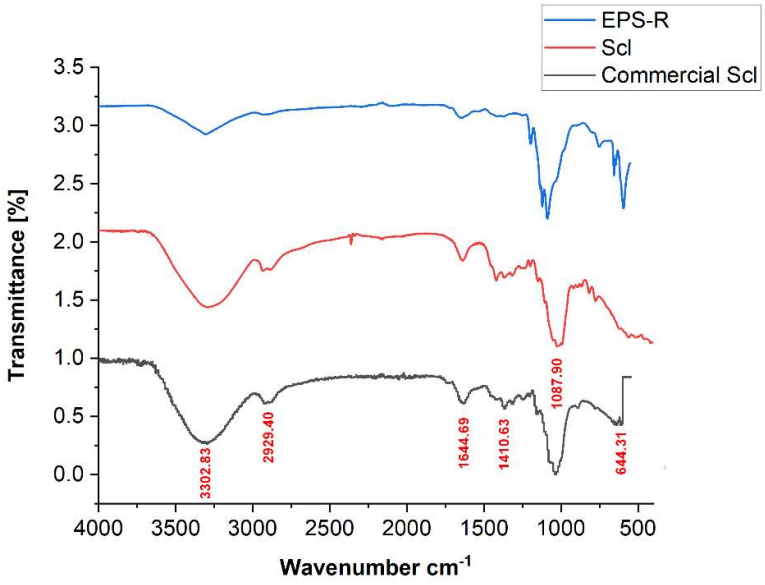
EPS-R
Scl
Commercial Scl
Transmittance [%]
Wavenumber cm-1
3302.83
2929.40
1644.69
1410.63
1087.90
644.31

Fig. 1

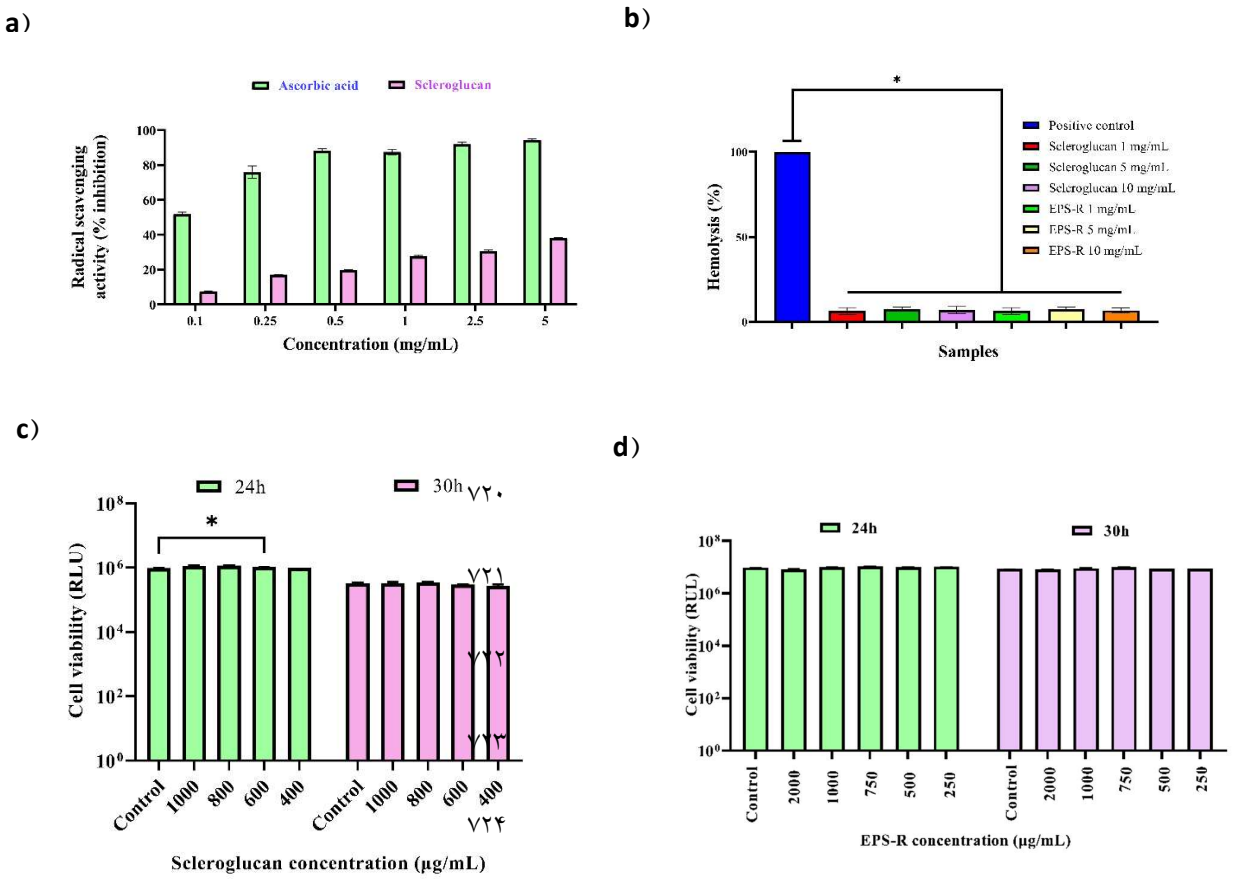
a)
Ascorbic acid
Scleroglucan
Radical scavenging activity (% inhibition)
Concentration (mg/mL)
b)
Positive control
Scleroglucan 1 mg/mL
Scleroglucan 5 mg/mL
Scleroglucan 10 mg/mL
EPS-R 1 mg/mL
EPS-R 5 mg/mL
EPS-R 10 mg/mL
Hemolysis (%)
Samples
c)
24h
30h
Cell viability (RLU)
Control
Scleroglucan concentration (µg/mL)
d)
24h
30h
Cell viability (RUL)
Control
EPS-R concentration (µg/mL)

Fig. 2

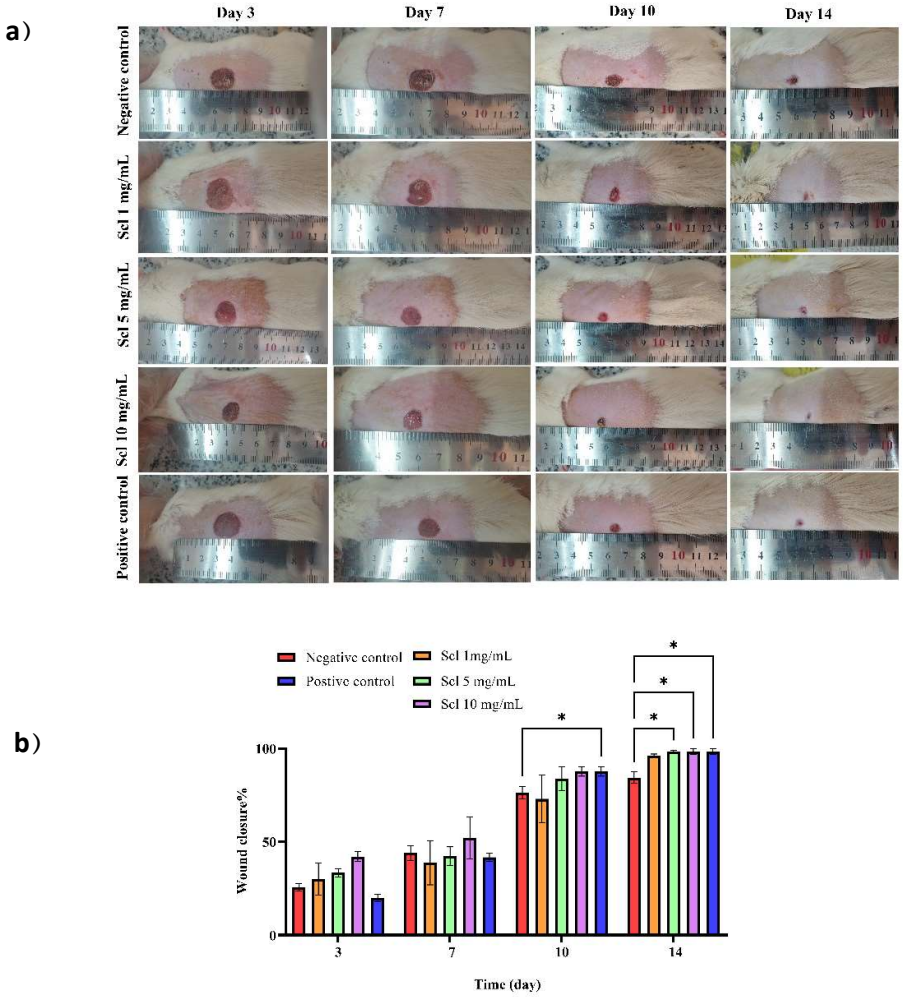
a)
Day 3
Day 7
Day 10
Day 14
Negative control
Scl 1 mg/mL
Scl 5 mg/mL
Scl 10 mg/mL
Positive control
b)
Negative control
Postive control
Scl 1mg/mL
Scl 5 mg/mL
Scl 10 mg/mL
Wound closure%
Time (day)
c)
40x
400x
Normal Skin
Negative Control
Scl 1 mg/mL
Scl 5 mg/mL
Scl 10 mg/mL
Positive Control
E
F
200 µm
20 µm

Fig. 3

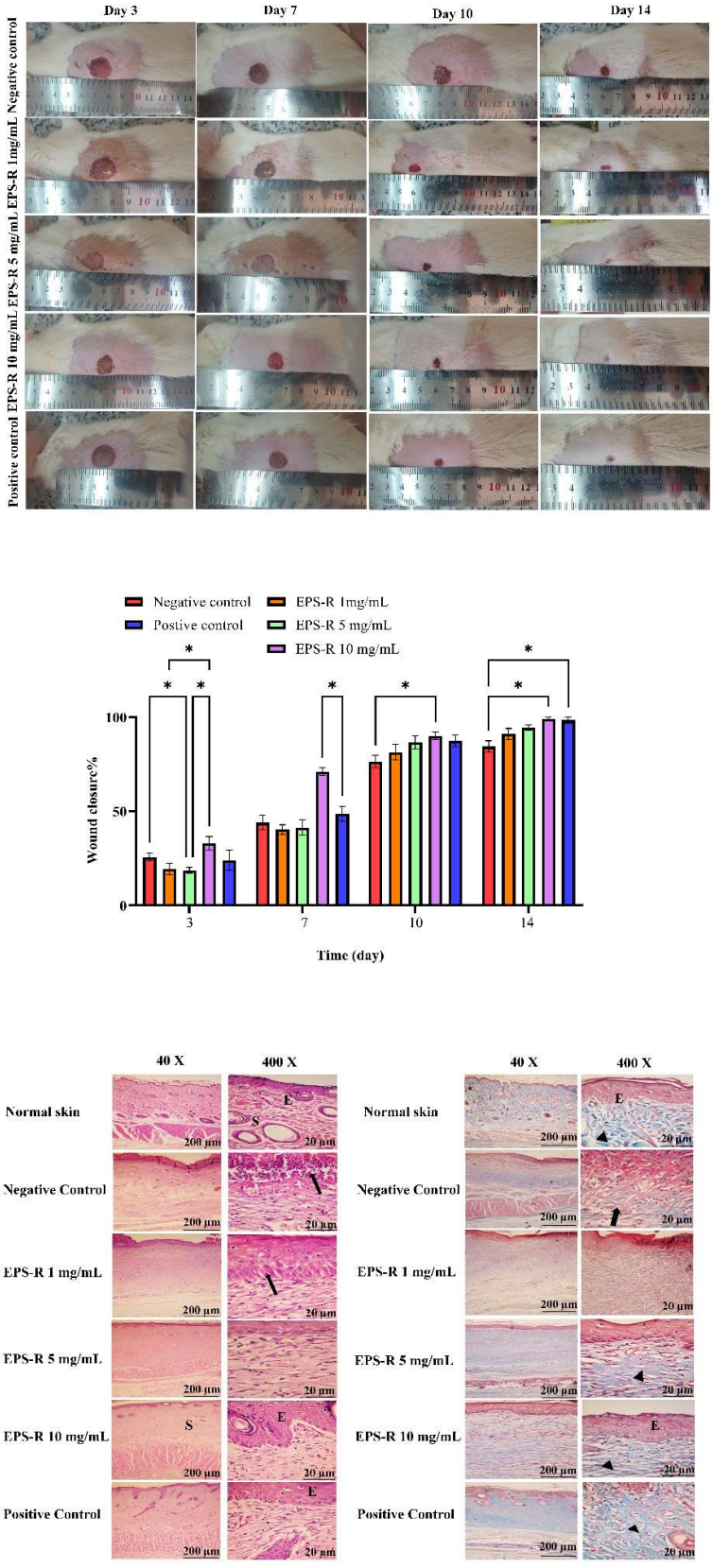
a)
Day 3
Day 7
Day 10
Day 14
Negative control
EPS-R 1mg/mL
EPS-R 5 mg/mL
EPS-R 10 mg/mL
Positive control
b)
Negative control
Postive control
EPS-R 1mg/mL
EPS-R 5 mg/mL
EPS-R 10 mg/mL
Wound closure%
Time (day)
c)
40 X
400 X
Normal skin
Negative Control
EPS-R 1 mg/mL
EPS-R 5 mg/mL
EPS-R 10 mg/mL
Positive Control
200 µm
20 µm
E
S

Fig. 4

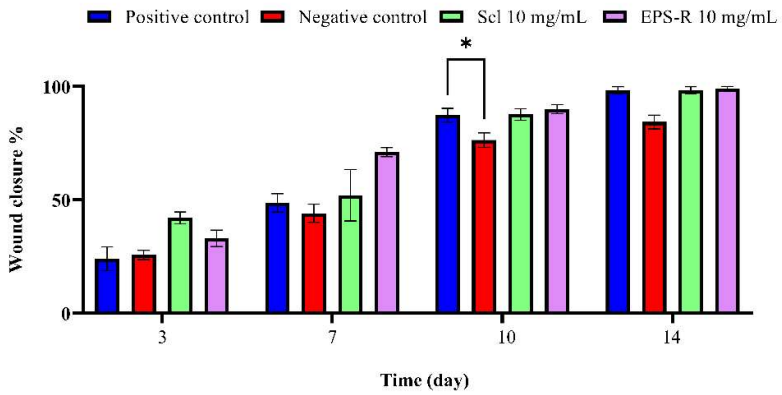
Positive control
Negative control
Scl 10 mg/mL
EPS-R 10 mg/mL
*
100
50
0
Wound closure %
3
7
10
14
Time (day)

Fig. 5